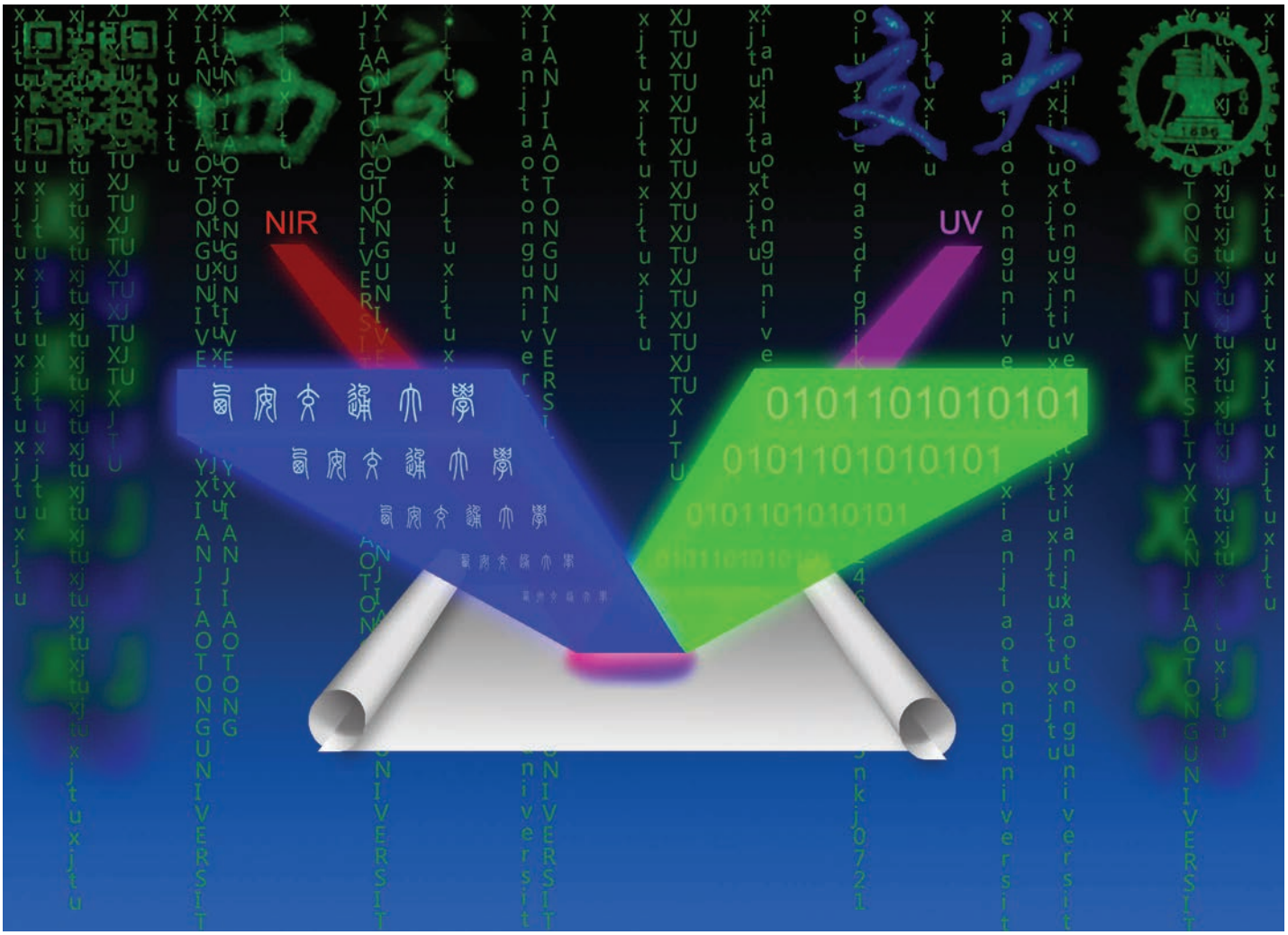

Showcasing research from the Bioinspired Engineering and Biomechanics Center (BEBC), Xi'an Jiaotong University, Xi'an, China.

Inkjet printing of upconversion nanoparticles for anti-counterfeit applications

Patterning upconversion luminescence materials have been widely used for anti-counterfeit and security applications. Here, we report a digital and flexible inkjet printing based approach for producing high-resolution and high-luminescence anti-counterfeit patterns. We achieved two different patterns in the same area, which show up separately under excitation by different wavelength laser sources. The developed technology is promising to carry an abundance of information and enhance anti-counterfeit technology.

As featured in:

See Min Lin, Feng Xu *et al*. *Nanoscale*, 2015, 7, 4423.

ROYAL SOCIETY OF CHEMISTRY

www.rsc.org/nanoscale

Registered charity number: 207890

Nanoscale

PAPER

View Article Online
View Journal | View Issue

Published on 05 January 2015. Downloaded by Xian Jiaotong University on 30/05/2016 13:17:43.

Cite this: *Nanoscale*, 2015, **7**, 4423

Inkjet printing of upconversion nanoparticles for anti-counterfeit applications†

Minli You,‡[a,b] Junjie Zhong,‡[b,c] Yuan Hong,[b,d] Zhenfeng Duan,[e] Min Lin*[a,b,e] and Feng Xu*[a,b]

Received 24th November 2014,
Accepted 3rd January 2015

DOI: 10.1039/c4nr06944g

www.rsc.org/nanoscale

Patterning of upconversion luminescent materials has been widely used for anti-counterfeit and security applications, where the preferred method should be easy, fast, multicolor, high-throughput and designable. However, conventional patterning methods are complex and inflexible. Here, we report a digital and flexible inkjet printing based approach for producing high-resolution and high-luminescence anti-counterfeit patterns. We successfully printed different multicolor luminescent patterns by inkjet printing of upconversion nanoparticles with controlled and uniform luminescence intensity through optimizing the inks and substrates. Combined with another downconversion luminescent material, we achieved two different patterns in the same area, which show up separately under excitation by different wavelength laser sources. The developed technology is promising to use one single substrate for carrying abundant information by printing multilayer patterns composed of luminescent materials with different excitation light sources.

1. Introduction

Anti-counterfeit technologies have found widespread applications in identity cards, currency, tags and important documents.[1,2] These applications have shown a significant importance for business and national public safety.[3] Especially with the rapid expansion of small business, sole traders and personal demands, there is an urgent need to develop a low cost, easily accessible, and personalized anti-counterfeit technology. To meet this emerging need, various anti-counterfeit technologies including laser holography,[4] nuclear track technology,[5] and luminescence printing[6] may be employed among which luminescence printing offers several advantages such as being high-throughput, designable and showing advanced anti-counterfeit performance. For luminescence-based anti-counterfeit, luminescent ink is used to produce various coded patterns and the anti-counterfeit property mainly results from two aspects, *i.e.* the high concealment luminescent materials[7] and the complex coded pattern.[8]

Both organic and inorganic luminescent materials based on the so-called 'downconversion' process (*e.g.*, photochromic compounds, semiconductor quantum dots, lanthanide doped oxides) have been used as luminescent ink,[1,9,10] which are featured by longer-wavelength visible emission when exposed to shorter-wavelength excitation, mostly ultraviolet (UV) light. However, UV-to-visible downconversion materials and UV excitation sources have become more accessible, making it much easier to duplicate. In contrast, near-infrared (NIR)-to-visible luminescent materials based on the so-called 'upconversion' luminescence are more difficult to duplicate as compared with UV-to-visible materials.[11–17] Besides, the NIR excitation sources are more difficult to access and will not excite standard downconversion luminescent materials, making it possible to print patterns on highly fluorescent surfaces (*e.g.*, papers and textiles with optical brighteners).[18] Moreover, upconversion materials can be formulated to produce the designed emission color only at specific excitation power densities[19] and the designed luminescence lifetime by controlling the ratio of Yb and Tm,[20,21] making it even more difficult to duplicate.

To produce complicated, elaborate and high-resolution upconversion luminescence patterns for anti-counterfeit applications, various printing technologies have been explored. Kim *et al.* have fabricated predefined patterns of upconversion

[a]*The Key Laboratory of Biomedical Information Engineering of Ministry of Education, School of Life Science and Technology, Xi'an Jiaotong University, Xi'an 710049, P.R. China. E-mail: fengxu@mail.xjtu.edu.cn*
[b]*Bioinspired Engineering and Biomechanics Center (BEBC), Xi'an Jiaotong University, Xi'an 710049, P.R. China. E-mail: minlin@mail.xjtu.edu.cn*
[c]*School of Energy and Power Engineering, Xi'an Jiaotong University, Xi'an 710049, P.R. China*
[d]*College of Life Sciences, Nanjing Agricultural University, Nanjing 210095, P.R. China*
[e]*Center for Sarcoma and Connective Tissue Oncology, Massachusetts General Hospital, Harvard Medical School, MA 02114, USA*
†Electronic supplementary information (ESI) available: SEM micrograph of A4 duplicating paper and vegetable parchment paper printed with(out) solvent based ink and aqueous ink. See DOI: 10.1039/c4nr06944g
‡The authors contributed equally.

Published on 05 January 2015. Downloaded by Xian Jiaotong University on 30/05/2016 13:17:43.

nanoparticles using a photolithography technique, which however involves a multi-step process.[14] To simplify the operating process, Blumenthal *et al.* developed a one-step printing process accompanied by Sono-Tek screen-printing and M3D direct-write printing process based on NIR-to-visible inks composed of β-$NaYF_4$:Yb^{3+}, Er^{3+} nanoparticles in a polymer matrix.[12] This study was further extended by Meruga *et al.* for the fabrication of multicolor two-dimensional codes visible only under NIR excitation using a new one-step printing process based on Aerosol Jet technology.[15,16] Although significant progress has been made, there are several limitations associated with these existing printing platforms. For example, a screen-printer can only print one-color ink in a single printing process. Although an aerosol jet printer provides high spatial resolution,[12] it is time consuming and complex to operate due to its huge and intricate structure. In addition, poly(methyl methacrylate) (PMMA) is used as an ink binding reagent to maintain the film uniformity in these printing systems.[12,16] This requires a time-consuming procedure to prepare both inks and substrates. Besides, the use of PMMA in the ink involves the potential issue of the 'coffee ring effect', which may result in fracture of printed patterns.[12] Therefore, developing an easy accessible, high-throughput, multicolor and designable printing method for upconversion-based anti-counterfeit applications is highly demanded.

To address the above-mentioned challenges, we applied inkjet printing for patterning inks composed of upconversion nanoparticles. Inkjet printing is versatile and high-throughput, and involves user-friendly processing steps. Inkjet printing has been widely used for the fabrication of many complex structures, including transistor circuits,[22–27] optical devices,[28–33] chemical sensors,[34–36] and so on. Its advanced applications can be attributed to its attractive features that include (1) the possibility for purely additive operation, in which the corresponding inks are deposited only where they are needed, (2) the flexibility in the choice of structure designs for producing complicated security patterns, where changes can be made rapidly using software-based printer-control systems (as shown in Fig. 1), (3) the compatibility with large-area substrates and (4) the potential for high spatial resolution (depending on the DPI) and mass production.[37] These advantages make inkjet-printing a prospective method for anti-counterfeit printing.

In this paper, we report the preparation of NIR-to-visible ink that is suitable for inkjet printing and multilayer pattern printing using luminescent materials with different excitation light sources. The developed method is capable of producing anti-counterfeit features, and is easy, fast, multicolor, high-throughput, designable and low cost. Essential characteristics of inks, substrates and the resulting patterns were studied. Contact angles between different inks and substrates were characterized to indicate the relationship with spatial resolution. In addition, the luminescence intensity and uniformity were tested to prove the high quality of printed patterns. With the help of a personal computer, we produced different types of two-dimensional patterns visible only under a 980 nm NIR excitation source. Furthermore, multilayer patterns were realized by printing an upconversion pattern (containing upconversion nanoparticles) over a downconversion pattern (containing a downconversion dye). No background luminescence interference was observed on the overlap area, which increases the coding complex and is essential for security purposes.

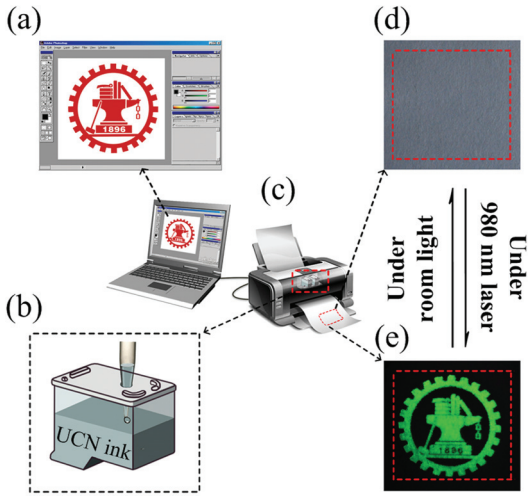

Fig. 1 Schematic of inkjet printing upconversion nanoparticles for anti-counterfeit applications. (a) Designing patterns on the computer using software. (b) Preparing the cartridge and UCNP ink. (c) Printing patterns using the inkjet printer connected with the computer. (d) Upconverting patterns exposed to room light. (e) Upconverting patterns exposed under a 980 nm laser.

2. Materials and methods

2.1. Materials

$YCl_3·6H_2O$, $YbCl_3·6H_2O$, $ErCl_3·6H_2O$, $TmCl_3·6H_2O$, and ammonium fluoride (NH_4F) were purchased from Sigma Aldrich. 1-Octacene (90%) sodium and oleic acid (90%) were obtained from Alfa Aesar. Methanol, glycerol (99.0%), chloroform, ethanol and sodium hydroxide (NaOH) were obtained from Tianjinzhiyuan Chemical Reagent Co., Ltd. Poly(acrylic acid) was obtained from Tianjinyongsheng Chemical Reagent Co., Ltd. Glycerol trioleate (60%) was purchased from Aladdin Chemistry Co., Ltd. Sodium dodecyl sulfonate (SDS) (90%) was obtained from ChengDu Kelong Chemical Co., Ltd. All reagents except for glycerol trioleate (chemically pure) were of analytical grade and were used without any purification. UV-Vis ink used here is #110UV Invisible Endorsing Noris Ink from NORIS USA Co., Ltd. Vegetable parchment was obtained from Suzhouguanhua Paper Factory. A4 duplicating paper was purchased from Double A (1991) Public Co., Ltd.

2.2. Synthesis of upconversion nanoparticles (UCNPs)

2.2.1 Synthesis of β-$NaYF_4$:Yb,Er/Tm nanoparticles. UCNPs were synthesized following the protocol from the literature.[38] In a typical synthesis of 30 nm sized β-$NaYF_4$:Er, Yb nanoparticles, $YCl_3·6H_2O$ (242.69 mg, 0.8 mmol), $YbCl_3·6H_2O$

 This journal is © The Royal Society of Chemistry 2015

Published on 05 January 2015. Downloaded by Xian Jiaotong University on 30/05/2016 13:17:43.

(69.75 mg, 0.18 mmol), and $ErCl_3{\cdot}6H_2O$ (7.64 mg, 0.02 mmol) dissolved in 2 mL deionized water were added to a 100 mL flask containing 7.5 mL oleic acid and 15 mL 1-octadecene. The solution was stirred at room temperature for 0.5 h. Then the mixture was slowly heated to 120 °C, kept for 1 h and then heated to 156 °C for another 1 h to remove water under an argon atmosphere. The system was then cooled down to room temperature. Then a 5 mL methanol solution of NH_4F (148.15 mg, 4 mmol) and NaOH (100 mg, 2.5 mmol) was added and the mixture was stirred at room temperature for 2 h. After methanol evaporation, the solution was heated to 280 °C and maintained for 1.5 h, then cooled down to room temperature. The resulting product was washed with ethanol and cyclohexane several times, and finally dispersed in cyclohexane for further use. Synthesis of $NaYF_4$:Yb,Tm nanocrystals was performed following a similar protocol by changing the molar ratio of the reagents, $YCl_3{\cdot}6H_2O$ (210.8 mg, 0.695 mmol), $YbCl_3{\cdot}6H_2O$ (116.2 mg, 0.30 mmol), and $TmCl_3{\cdot}6H_2O$ (1.9 mg, 0.005 mmol).

2.2.2 Surface modification. A ligand exchange process was performed using poly(acrylic acid) (PAA, M_w = 1800) as a multidentate ligand which displaces the original hydrophobic ligands on the UNCP surface by mixing together 14.5 μl PAA, 1 ml ethanol and 1 mL of UCNP dispersion in chloroform (15 mg ml^{-1}) with overnight stirring. The solution was then centrifuged at 10 000 rpm for 10 min. After washing 3 times with ethanol and DI water, the particles can be re-dispersed well in water.

2.3. Ink formulation

2.3.1 Preparation of hydrophobic printing ink. UCNPs were added to a cyclohexane and glycerol trioleate solution with ratio (in volume) of 90 : 10 to 70 : 30 for obtaining ink with the optimal performance, such as viscosity and surface tension. The resulting mixture was then stirred for 10 minutes, followed by 10 minutes of sonication to achieve complete dissolution of nanoparticles.

2.3.2 Preparation of hydrophilic printing ink. UCNPs after surface modification were added to a ethanol (10%) and glycerol solution with ratio (in volume) of 85 : 15 to 65 : 35 for obtaining a specific range of dynamic viscosity required for different printers. SDS was then added at a concentration of 3 mg l^{-1} to control the surface tension of ink. The resulting mixture was then vigorously stirred for 20 minutes, followed by 20 minutes of sonication to achieve complete dissolution of nanoparticles.

2.4. Equipment and characterization

The printing was performed with a modified HP Deskjet 1000 inkjet printer. The dynamic viscosity of ink was measured using a Pinkevitch Viscometer (Shenyangzhongya Glassware Instrument Co., Ltd) with a 0.6 mm diameter capillary tube and the surface tension was measured with capillary tubes (West China University of Medical Science Instrument Factory) of 0.3 mm diameter. The morphologies of the samples were obtained by high-resolution transmission electron microscopy (HRTEM) using a JEM 2100 instrument at an accelerating voltage of 200 kV. The as-prepared samples were characterized by powder X-ray diffraction (XRD) on an XRD-7000 diffractometer with Cu K_α radiation. The FT-IR spectra of the nanoparticles were obtained using a Nicolet iS50 Fourier transform infrared spectrophotometer (Thermo Electron Co., USA) by the KBr method. The upconversion emission spectra were recorded by using a spectrophotometer (QuantaMasterTM40) under external excitation of a 250 mW 980 nm laser diode (RGB Lasersystems). Images of printed patterns upon excitation using a 980 nm CW laser (Changchun Liangli Photoelectric Co., Ltd) were obtained *via* a Nikon D90 digital Single Lens Reflex with Macro lens and an attached UV/IR filter. All the measurements were performed at room temperature.

3. Results and discussion

3.1. β-$NaYF_4$:Yb,Er nanoparticles

A uniform and high-luminescence pattern requires that the ink composed of fluorescent nanoparticles should possess good solubility and high luminescence intensity. The $NaYF_4$:Yb,Er nanoparticles used as an ink component in this study were synthesized by a thermal decomposition route in the presence of oleic acid (OA) and octadecene, as modified from procedures described previously.[38,39] To produce two different polar inks, we prepared hydrophobic nanoparticles, OA-UCNPs (Fig. 2a), and PAA modified hydrophilic nanoparticles, PAA-UCNPs (Fig. 2b). The OA-UCNPs can be easily dispersed in a nonpolar solvent such as cyclohexane, with a mean diameter of 25.8 nm (Fig. 2a), which is suitable for smooth printing of this cartridge. The PAA-UCNPs are water-soluble and remain monodispersed with almost unchanged particle size and shape as compared with OA-UCNPs (Fig. 2a, b). The XRD pattern of the product shows that all the diffraction peaks can be ascribed to the hexagonal structure of $NaYF_4$ (JCPDS

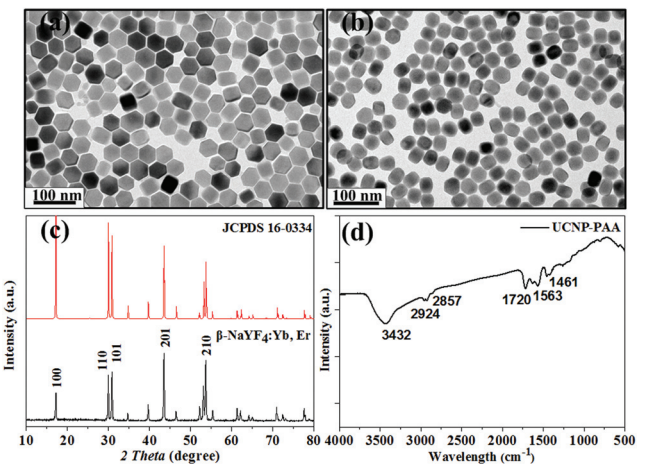

Fig. 2 Characterization of the UCNPs. TEM image of β-$NaYF_4$:Er,Yb nanoparticles (a) before and (b) after PAA modification. (c) Powder XRD of the β-$NaYF_4$:Er,Yb nanocrystal sample compared to ICDD PDF card for β-$NaYF_4$. (d) FT-IR spectrum of PAA capped β-$NaYF_4$:Er,Yb.

Published on 05 January 2015. Downloaded by Xian Jiaotong University on 30/05/2016 13:17:43.

no.16-0334) (Fig. 2c). It is reported that hexagonal phase (β-$NaYF_4$:Yb,Er) nanoparticles possess higher upconversion efficiency than cubic phase (α-$NaYF_4$:Yb,Er) nanoparticles.[40] The capping ligands on the surface of UCNPs were identified by FT-IR spectroscopy (Fig. 2d). The PAA modified UCNP samples exhibit a broad band at approximately 3432 cm^{-1}, corresponding to the O–H stretching vibration. The transmission bands at 2924 and 2857 cm^{-1} can be assigned to the asymmetric and symmetric stretching vibrations of the methylene (CH_2) in the long alkyl chain, respectively. Two strong bands centered at 1563 and 1461 cm^{-1} are observed, which can be associated with the asymmetric and symmetric stretching vibrations of carboxylate anions on the surface of the NPs, respectively. Meanwhile, the strong band at 1720 cm^{-1} indicates the presence of the COOH groups on the particle surface. Therefore, it can be concluded that PAA has successfully bonded to the UCNP surface.[41] Furthermore, to generate ink droplets in a controllable manner and to avoid printing instability (*e.g.*, clustering of the particles at the nozzle edge, deviation of the drop trajectory, agglomerates blocking the nozzle), the size of the ink components (*i.e.*, dispersed molecules or nanoparticles) should be less than 1/50 of the nozzle diameter.[27] Here the diameters of nozzles used are over 10 μm, requiring a suitable nanoparticle size of less than 200 nm. Therefore, the upconversion nanoparticles we synthesized entirely meet these criteria.

3.2. Inkjet properties

3.2.1 Ink properties. To ensure that inks work stably on the inkjet printer and optimize the printing resolution and luminescence intensity, we tuned ink properties by evaluating the printing performance (*i.e.*, dynamic viscosity and surface tension). When ink drops land on a substrate, the flow of liquid drops would affect the printing resolution. The spreading of the liquid drops could be measured using the inverse Ohnesorge number, $Z = \sqrt{\gamma\rho\alpha}/\eta$, with nozzle diameter α, and surface tension γ, density ρ, and dynamic viscosity η.[31] To achieve uniform and high-resolution patterns, we adjusted Z ranging between 4.2 and 11.0 for the solvent based printing ink, and between 5.8 and 13.1 for the aqueous printing ink, which match reported data.[27] Here the dynamic viscosity and surface tension are the critical parameters for the printing performance. The dynamic viscosity of ink also affects its flow in the cartridge and through the nozzle, where high viscosity ink may result in nozzle clogging while low viscosity ink may induce damped oscillations in the jet resulting in an inhomogeneous droplet size. Besides, low viscosity ink is able to infiltrate through micropores between fibers of substrates, leading to a situation that only a little ink adheres to the surface of the substrate, thereby decreasing the luminescence intensity of patterns under NIR excitation. In addition, an appropriate surface tension of ink helps in keeping a relatively small contact angle over substrates, which increases the coverage area for a single drop of ink to form patterns with good uniformity under certain dots per inch (DPI) of a printer. The preferred dynamic viscosity and surface tension of ink for the inkjet printer may vary within a specific range at room temperature: the dynamic viscosity varies from 1 to 5 mPa s (cp) while the surface tension varies from 20 to 60 mN m^{-1} (dynes cm^{-1}).[42–48]

To prepare ink with the preferred parameters mentioned above, we adjusted ink components and their ratios. Organic solvent based or aqueous inks for different substrates were prepared with controlled dynamic viscosity and surface tension. Solvent based ink was prepared with cyclohexane (η equals to 0.886 mPa s and γ equals to 24.4 mN m^{-1}, 25 °C), which was used to disperse UCNPs, and glycerol trioleate (η equals to 37.8 mPa s and γ equals to 34.7 mN m^{-1}, 25 °C), which was suitable for preparing a mixture with moderate viscosity and surface tension. The obtained dynamic viscosity and surface tension change as a function of the ratio between cyclohexane and glycerol trioleate (Fig. 3a, b). A similar result was obtained with the aqueous printing ink (Fig. 3c, d). We dissolved glycerol (η equals to 945 mPa s and γ equals to 63.3 mN m^{-1}, 25 °C) and SDS into an ethanol–water solution (η equals to 1.04 mPa s and γ equals to 64.8 mN m^{-1}, 25 °C). The obtained dynamic viscosity and surface tension are within the range mentioned above (Fig. 3c, d). Compared to previous reported methods,[12–14,16] both the ink components and the preparation procedures are easier for operation and mass production. This demonstrates the advantage in using the inkjet printer by applying UCNPs for high-throughput security printing.

3.2.2 Contact angle and spatial resolution. To further optimize the spatial resolution, we controlled the behavior of the ejected drop on the substrate, which can be described by fluid dynamics. When a liquid droplet lands on a flat surface,

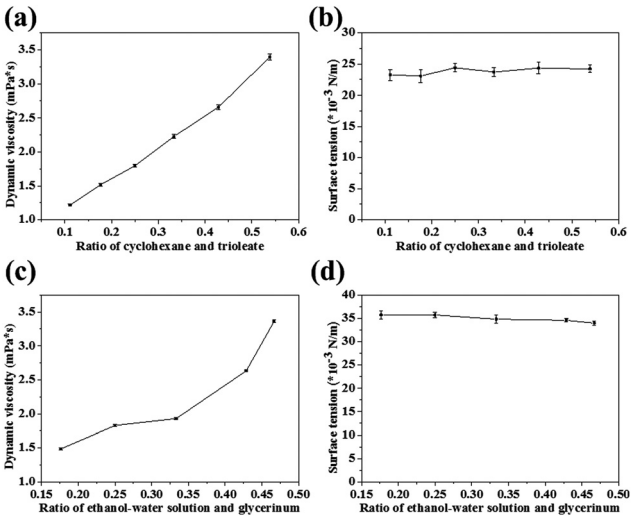

Fig. 3 Characterization of the UCNP ink with varying ratios of components at 25 ± 1 °C. (a) The dynamic viscosity of solvent based printing ink changes with the v : v cyclohexane : glycerol trioleate ratio. (b) The gas–liquid surface tension of solvent based printing ink changes with the v : v cyclohexane : glycerol trioleate ratio. (c) The dynamic viscosity of aqueous printing ink changes with v : v ethanol–water solution(10%) : glycerol ratio. (d) The gas–liquid surface tension of aqueous printing ink changes with the v : v ethanol–water solution(10%) : glycerol ratio.

 This journal is © The Royal Society of Chemistry 2015

Published on 05 January 2015. Downloaded by Xian Jiaotong University on 30/05/2016 13:17:43.

partial wetting results in a finite angle between the liquid and the substrate, known as the contact angle, θ_c.[27] This parameter affects the penetration of ink into substrates which can be described by Washburn's equation: $L = \sqrt{\gamma D_t \cos\theta_c}/(4\eta)$, where γ is the surface tension, D is the diameter of the capillary tube (capillary porosity between paper fibers), θ_c is the contact angle, and η is the dynamic viscosity. The quality of printed patterns is mainly affected by different contact angles formed when inks drop on the substrates. Since various substrates possess different capillary porosities and produce different contact angles, studying their influences on patterns printed is of essential importance. For this, we printed solvent based and aqueous inks separately onto A4 duplicating and vegetable parchment to demonstrate the relationship between the contact angle and the spatial resolution of patterns. The microstructure of the printed papers was analyzed by SEM and is shown in Fig. S1.†

Solvent based and aqueous inks were applied to print a series of parallel lines with an equal width and interval. When solvent based and aqueous ink dropped on a piece of A4 duplicating paper (80 g m^{-2}, white color, purchased from Double A (1991) Public Co., Ltd), they displayed slightly different droplet morphologies which can be reflected by the contact angle. After five parallel tests, the contact angle of the solvent based printing ink was 25.7 ± 0.8 degrees and that of the aqueous ink was 32.8 ± 1.2 degrees (Fig. 4a, b). Although there is ~21.6% diversity between these two contact angles, printed patterns are of similar spatial resolution as indicated by a series of clear parallel lines of 200 μm equal width and interval (Fig. 4a, b). In contrast, when dropping on a piece of vegetable parchment (83 g m^{-2}, white color, purchased from Suzhouguanhua Paper Factory), there exists a significant variance in the contact angle between two kinds of inks with 9.0 ± 0.6 degrees for solvent based ink and 52.7 ± 1.3 degrees for aqueous ink. As we know, vegetable parchment is hydrophobic, so a large contact angle can remain between aqueous ink and the vegetable parchment surface, but it is not the case for solvent based ink. In this situation, the spatial resolution printed using aqueous printing ink is 100–200 μm and using solvent based ink is 400–500 μm (Fig. 4c, d). In summary, spatial resolution is directly related to the contact angle. A larger contact angle corresponds to higher spatial resolution of printed patterns. As described above, different polarity between the ink and the substrate facilitates the formation of a larger contact angle resulting in higher spatial resolution. As compared with solvent based ink, aqueous ink shows higher spatial resolution no matter on A4 paper or on vegetable paper. Aqueous ink is more stable than solvent based ink, and is less apt to the block printer, holding great potential for further applications.

Compared with screen printing[12,13] and aerosol jet printer,[12,15,16] the developed inkjet printing provides higher spatial resolution of less than 200 μm (Fig. 4d). Furthermore, the HP Deskjet 1000 printer applied in this study has a black-and-white DPI of 600 × 600. Therefore, the spatial resolution can be further improved when using an inkjet printer with higher DPI or using a color cartridge (802 tri-color cartridge). It is noteworthy that the HP Deskjet 1000 inkjet printer applied in our experiment possesses a theoretical black-and-white printing speed of ~12 pages per minute (PPM),[49] which is faster than other printing techniques studied before in printing complex two-dimensional patterns.[12,16]

3.3. Luminescence intensity and uniformity

Identification of printed patterns depends mainly on the luminescence uniformity which is affected by the size and distri-

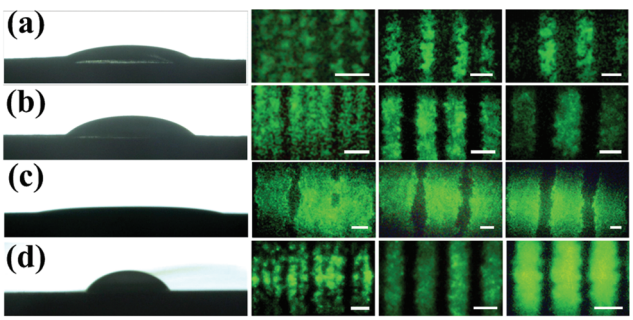

Fig. 4 Characterization of the spatial resolution of printing. (a) Droplet morphology of solvent based printing ink on A4 duplicating paper and equal interval and width (from left to right, 100 μm, 200 μm, 300 μm) lines printed. (b) Droplet morphology of aqueous printing ink on A4 duplicating paper and equal interval and width (from left to right, 100 μm, 200 μm, 300 μm) lines printed. (c) Droplet morphology of solvent based printing ink on vegetable parchment and equal interval and width (from left to right, 400 μm, 500 μm, 600 μm) lines printed. (d) Droplet morphology of aqueous printing ink on vegetable parchment and equal interval and width (from left to right, 100 μm, 200 μm, 300 μm) lines printed. The scale bar of each represents 300 μm.

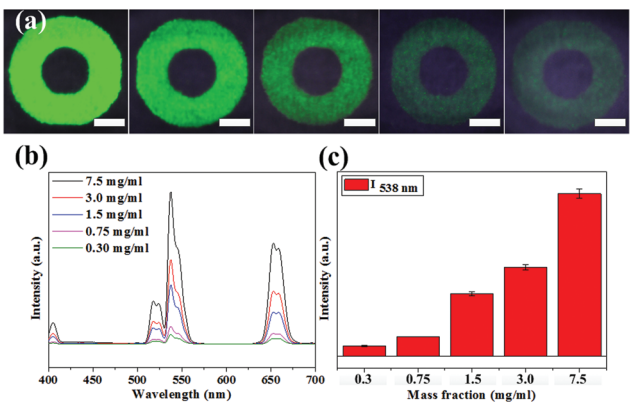

Fig. 5 Characterization of luminescence intensity and uniformity. (a) Luminescence changes along with the change of the UCNP concentration (from left to right 7.5 mg ml^{-1}, 3.0 mg ml^{-1}, 1.5 mg ml^{-1}, 0.75 mg ml^{-1}, 0.3 mg ml^{-1}). Patterns are explored under a 980 nm laser, with a power density of ~50 mW mm^{-2}. Figures are obtained using a Nikon D90 camera under f 5.8 (aperture) and 6 s (shutter duration) conditions. (b) Luminescence spectrum of different mass fractions of UCNPs. (c) Variance of the luminescence intensity at 538 nm wavelength of ring printing areas with different mass fractions of UCNPs. The scale bar of each represents 2 mm.

Published on 05 January 2015. Downloaded by Xian Jiaotong University on 30/05/2016 13:17:43.

bution of droplets from the nozzle. Therefore, to verify the luminescence uniformity of printed patterns by our printing system, we tested the variance of the luminescence intensity in a ring printing area with different UCNP concentrations varying from 0.3 mg ml^{-1} to 7.5 mg ml^{-1} under 980 nm excitation with a power density of ~50 mW mm^{-2} (Fig. 5a). For each concentration, we randomly tested the luminescence intensity of five points from the printing area. The corresponding luminescence spectrum of UCNPs with different concentrations under 980 nm excitation and the deviation in the luminescence intensity peaking at 538 nm are shown in Fig. 5b and c. We did not observe any significant difference in the luminescence intensity (<10% deviation).

3.4. Application prospect

3.4.1 Multicolor pattern. When changing the dopant element types or their ratio, UCNPs are able to emit different colors of light under NIR excitation.[50–52] It is therefore promising to print multicolor anti-counterfeiting patterns using UCNPs. Studies concerning multicolor upconversion luminescence patterns have been reported previously using a complex aerosol-jet printer.[15] Here we aimed at demonstrating the easy access of producing multicolor upconversion luminescence patterns using an inkjet printer. We applied two colors of inks composed of UCNPs with different color emission (green, β-$NaYF_4$:Yb,Er and blue, β-$NaYF_4$:Yb,Tm). The printed patterns are shown in Fig. 6. The acronym of Xi'an Jiao Tong University was patterned by the inkjet printer and exposed to a 980 nm NIR laser, where "X J" was printed with green ink and "T U" with blue ink (Fig. 6a). Since these two kinds of inks were able to be printed and excited to display different colors, providing the potential to produce multicolor patterns using different color inks as designed by switching cartridges or using color cartridges of the inkjet printer. Moreover, recently a cheap and flexible patterning way has been developed that directly wrote ink on paper using a pen. This method is fitted for simple patterns and for patterning various functional materials.[53–56] To further decrease the cost and simplify the process to a more easy operating way, we directly wrote Chinese characters with a pen filled with two color inks, green and blue. We observed three clear and bright characters on an A4 paper under 980 nm NIR excitation (Fig. 6c, d). This design is promising for personalized security information or signature.

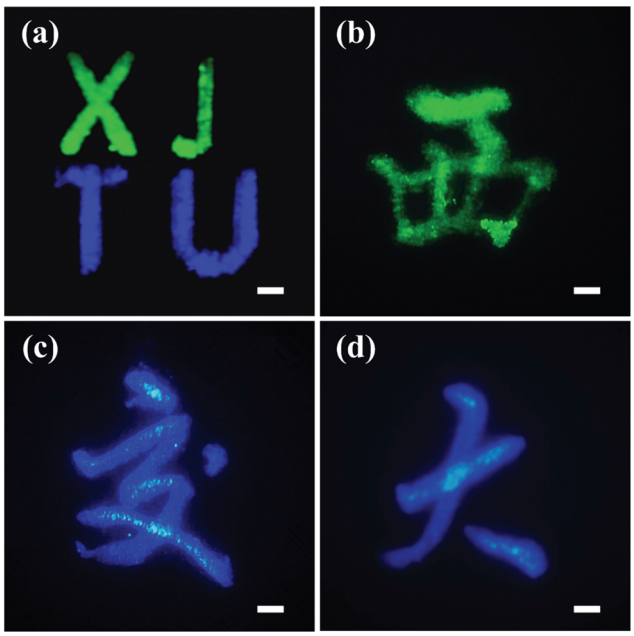

Fig. 6 Multicolor patterning of $NaYF_4$:Yb,Er (green) and $NaYF_4$:Yb,Tm (blue) by direct-writing with a pen. (a) Printed acronym of Xi'an Jiao Tong University, where "X J" is printed with green ink and "T U" with blue ink. (b)Written with green ink and (c) and (d) with blue ink. All pictures obtained under a 980 nm NIR laser source. The scale bar represents 1 mm.

3.4.2 Double anti-counterfeiting pattern. UV-to-visible downconversion security inks are widely used to produce counterfeit items including identity cards, currency and important documents. However, it always suffers from the appearance of duplications, since UV-to-visible downconversion inks and UV excitation sources have become much easier to obtain, while the NIR-to-visible upconversion inks and the NIR excitation source and reader are more difficult to access. Moreover, the NIR excitation source cannot excite standard downconversion luminescent materials, making it possible to print patterns on a highly luminescent surface.[18] Therefore, generation of different luminescence patterns that can be excited either by UV or NIR sources will reduce the possibility of counterfeits. For this purpose, we applied both UV-to-visible and NIR-to-visible inks for security printing. An A4 paper printed with both NIR-to-visible and UV-to-visible inks was exposed to room light, which clearly shows that nothing could be identified with naked eyes or cameras (Fig. 7a). When excited by a NIR light source, a two-dimensional code was seen clearly without

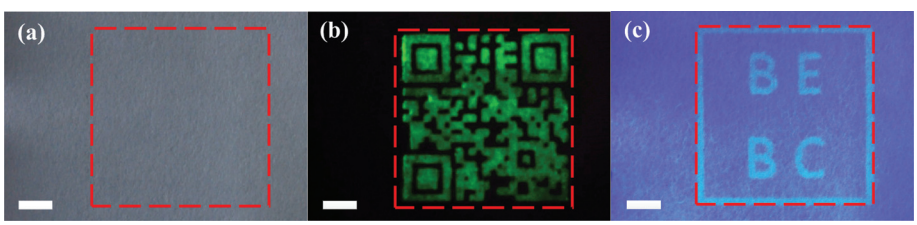

Fig. 7 Double anti-counterfeiting pattern. (a) Area of both NIR-to-visible and UV-to-visible printing features. (b) Two-dimensional code printed using NIR-to-visible upconversion ink. (c) 'BEBC' mark printed using UV-to-visible downconversion ink. The scale bar represents 2 mm.

 This journal is © The Royal Society of Chemistry 2015

Published on 05 January 2015. Downloaded by Xian Jiaotong University on 30/05/2016 13:17:43.

any other interference pattern (Fig. 7b). On substituting the NIR light source with a UV light source, a mark 'BEBC' was visualized in the same area, while the two-dimensional code printed using NIR-to-visible ink disappeared (Fig. 7c).

4. Conclusions

In summary, we report an easy, fast, multicolor, high-throughput, designable and low cost inkjet printing of upconversion nanoparticles for personal anti-counterfeit and security applications. We synthesized hexagonal phase nanoparticles with high upconversion efficiency and applied them to form two color printing inks. The dynamic viscosity and surface tension of ink are optimized within a specific range at room temperature. In addition, we found that there was a direct relationship between spatial resolution and contact angle. A larger contact angle contributes to higher spatial resolution of printed patterns. Moreover, the luminescence intensity under the same power density laser excitation can be adjusted by changing the UCNP concentration in ink, and there was at most 10% deviation in the luminescence intensity within a single concentration. Lastly, we utilized this upconversion luminescent inkjet printing system to print multicolor patterns and double anti-counterfeit patterns, which proves its promising applications for personalized anti-counterfeit and information security. The developed method can make anti-counterfeit marks feasible to produce and hard to duplicate, significantly enhancing the ability to anti-counterfeit.

Acknowledgements

This work was financially supported by the Major International Joint Research Program of China (11120101002), the International Science & Technology Cooperation Program of China (2013DFG02930), National Key Scientific Apparatus Development of Special Item (2013YQ190467), and the Fundamental Research Funds for the Central Universities (2012jdhz46). Min Lin is supported by a scholarship from the China Scholarship of Council. Feng Xu was also partially supported by the China Young 1000-Talent Program and the Program for New Century Excellent Talents in University. The TEM work was done at International Center for Dielectric Research (ICDR), Xi'an Jiaotong University, Xi'an, China. The authors also thank Ms Lu Lu and Mr Ma Chuan Sheng for their help in using TEM.

Notes and references

1 B. Yoon, J. Lee, I. S. Park, S. Jeon, J. Lee and J.-M. Kim, Recent functional material based approaches to prevent and detect counterfeiting, *J. Mater. Chem. C*, 2013, **1**(13), 2388–2403.
2 Y. Liu, K. Ai and L. Lu, Designing lanthanide-doped nanocrystals with both up- and down-conversion luminescence for anti-counterfeiting, *Nanoscale*, 2011, **3**(11), 4804–4810.
3 Y. Cui, R. S. Hegde, I. Y. Phang, H. K. Lee and X. Y. Ling, Encoding molecular information in plasmonic nanostructures for anti-counterfeiting applications, *Nanoscale*, 2014, **6**(1), 282–288.
4 T. Jin, W. Meng, S. Yan and M. Zhao, Method for producing laser hologram anti-counterfeit mark with identifying card and inspecting card and inspecting apparatus for the mark, *U.S. Patent*, 6,001,510[P], 1999-12-14.
5 Y. Yushun, H. Xiangming and Z. Quanrong, Breakthrough in fake prevention. Nuclear track-etching, *Physics*, 1999, **28**(5), 295–298.
6 J. Andres, R. D. Hersch, J.-E. Moser and A.-S. Chauvin, A New Anti-Counterfeiting Feature Relying on Invisible Luminescent Full Color Images Printed with Lanthanide-Based Inks, *Adv. Funct. Mater.*, 2014, **24**(32), 5029–5036.
7 P. Kumar, J. Dwivedi and B. K. Gupta, Highly-luminescent dual mode rare-earth nanorods assisted multi-stage excitable security ink for anti-counterfeiting applications, *J. Mater. Chem. C*, 2014, **2**(48), 10468–10475.
8 V. J. Cadarso, S. Chosson, K. Sidler, R. D. Hersch and J. Brugger, High-resolution 1D moires as counterfeit security features, *Light Sci. Appl.*, 2013, **2**, e86.
9 B. K. Gupta, D. Haranath, S. Saini, V. N. Singh and V. Shanker, Synthesis and characterization of ultra-fine Y2O3:Eu3+ nanophosphors for luminescent security ink applications, *Nanotechnology*, 2010, **21**(5), 055607.
10 T. K. Anh, D. X. Loc, T. T. Huong and N. Vu, Luminescent nanomaterials containing rare earth ions for security printing, *Int. J. Nanotechnol.*, 2011, **8**(3), 335–346.
11 N. M. Sangeetha, P. Moutet, D. Lagarde, G. Sallen, B. Urbaszek, X. Marie, *et al.* 3D assembly of upconverting NaYF4 nanocrystals by AFM nanoxerography: creation of anti-counterfeiting microtags, *Nanoscale*, 2013, **5**(20), 9587–9592.
12 T. Blumenthal, J. Meruga, M. P. Stanley, J. Kellar, W. Cross, K. Ankireddy, *et al.* Patterned direct-write and screen-printing of NIR-to-visible upconverting inks for security applications, *Nanotechnology*, 2012, **23**(18), 185305.
13 W. Cross, T. Blumenthal, J. Kellar, P. S. May, J. Meruga and Q. Luu, Rare-Earth Doped Nanoparticles in Security Printing Applications, *MRS Proceedings*, 2012, 1471.
14 W. J. Kim, M. Nyk and P. N. Prasad, Color-coded multilayer photopatterned microstructures using lanthanide(III) ion co-doped NaYF4 nanoparticles with upconversion luminescence for possible applications in security, *Nanotechnology*, 2009, **20**(18), 185301.
15 J. M. Meruga, A. Baride, W. Cross, J. J. Kellar and P. S. May, Red-green-blue printing using luminescence-upconversion inks, *J. Mater. Chem. C*, 2014, **2**(12), 2221–2227.
16 J. M. Meruga, W. M. Cross, M. P. Stanley, Q. Luu, G. A. Crawford and J. J. Kellar, Security printing of covert quick response codes using upconverting nanoparticle inks, *Nanotechnology*, 2012, **23**(39), 395201.
17 Y. Bao, Q. A. N. Luu, Y. Zhao, H. Fong, P. S. May and C. Jiang, Upconversion polymeric nanofibers containing lanthanide-doped nanoparticles via electrospinning, *Nanoscale*, 2012, **4**(23), 7369–7375.

Published on 05 January 2015. Downloaded by Xian Jiaotong University on 30/05/2016 13:17:43.

18 R. Ma, E. Bullock, P. Maynard, B. Reedy, R. Shimmon, C. Lennard, *et al.* Fingermark detection on non-porous and semi-porous surfaces using $NaYF_4$: Er, Yb up-converter particles, *Forensic Sci. Int.*, 2011, **207**(1), 145–149.

19 J. Zhao, D. Jin, E. P. Schartner, Y. Lu, Y. Liu, A. V. Zvyagin, *et al.* Single-nanocrystal sensitivity achieved by enhanced upconversion luminescence, *Nat. Nanotechnol.*, 2013, **8**(10), 729–734.

20 J. Zhao, Z. Lu, Y. Yin, C. McRae, J. A. Piper, J. M. Dawes, *et al.* Upconversion luminescence with tunable lifetime in NaYF4:Yb,Er nanocrystals: role of nanocrystal size, *Nanoscale*, 2013, **5**(3), 944–952.

21 Y. Lu, J. Zhao, R. Zhang, Y. Liu, D. Liu, E. M. Goldys, *et al.* Tunable lifetime multiplexing using luminescent nanocrystals, *Nat. Photonics*, 2014, **8**(1), 32–36.

22 H. Sirringhaus, T. Kawase, R. H. Friend, T. Shimoda, M. Inbasekaran, W. Wu, *et al.* High-Resolution Inkjet Printing of All-Polymer Transistor Circuits, *Science*, 2000, **290**(5499), 2123–2126.

23 H. S. Kim, J. S. Kang, J. S. Park, H. T. Hahn, H. C. Jung and J. W. Joung, Inkjet printed electronics for multifunctional composite structure, *Compos. Sci. Technol.*, 2009, **69**(7–8), 1256–1264.

24 H.-Y. Tseng, B. Purushothaman, J. Anthony and V. Subramanian, High-speed organic transistors fabricated using a novel hybrid-printing technique, *Org. Electron.*, 2011, **12**(7), 1120–1125.

25 H.-Y. Tseng and V. Subramanian, All inkjet-printed, fully self-aligned transistors for low-cost circuit applications, *Org. Electron.*, 2011, **12**(2), 249–256.

26 J. Perelaer, R. Abbel, S. Wünscher, R. Jani, T. van Lammeren and U. S. Schubert, Roll-to-Roll Compatible Sintering of Inkjet Printed Features by Photonic and Microwave Exposure: From Non-Conductive Ink to 40% Bulk Silver Conductivity in Less Than 15 Seconds, *Adv. Mater.*, 2012, **24**(19), 2620–2625.

27 F. Torrisi, T. Hasan, W. Wu, Z. Sun, A. Lombardo, T. S. Kulmala, *et al.* Inkjet-Printed Graphene Electronics, *ACS Nano*, 2012, **6**(4), 2992–3006.

28 K. W. Song, R. Costi and V. Bulovic, Electrophoretic Deposition of CdSe/ZnS Quantum Dots for Light-Emitting Devices, *Adv. Mater.*, 2013, **25**(10), 1420–1423.

29 M. Böberl, M. V. Kovalenko, S. Gamerith, E. J. W. List and W. Heiss, Inkjet-Printed Nanocrystal Photodetectors Operating up to 3 μm Wavelengths, *Adv. Mater.*, 2007, **19**(21), 3574–3578.

30 H. M. Haverinen, R. A. Myllylä and G. E. Jabbour, Inkjet Printed RGB Quantum Dot-Hybrid LED, *J. Disp. Technol.*, 2010, **6**(3), 87–89.

31 D. J. Finn, M. Lotya, G. Cunningham, R. J. Smith, D. McCloskey, J. F. Donegan, *et al.* Inkjet deposition of liquid-exfoliated graphene and MoS2 nanosheets for printed device applications, *J. Mater. Chem. C*, 2014, **2**(5), 925–932.

32 G. Hernandez-Sosa, S. Tekoglu, S. Stolz, R. Eckstein, C. Teusch, J. Trapp, *et al.* The compromises of printing organic electronics: a case study of gravure-printed light-emitting electrochemical cells, *Adv. Mater.*, 2014, **26**(20), 3235–3240.

33 K. Minxuan, W. Jingxia, B. Bin, L. Fengyu, W. Libin, J. Lei, *et al.* Inkjet Printing Patterned Photonic Crystal Domes for Wide Viewing-Angle Displays by Controlling the Sliding Three Phase Contact Line, *Adv. Opt. Mater.*, 2014, **2**(1), 34–38.

34 K. Abe, K. Suzuki and D. Citterio, Inkjet-Printed Microfluidic Multianalyte Chemical Sensing Paper, *Anal. Chem.*, 2008, **80**(18), 6928–6934.

35 V. Dua, S. P. Surwade, S. Ammu, S. R. Agnihotra, S. Jain, K. E. Roberts, *et al.* All-organic vapor sensor using inkjet-printed reduced graphene oxide, *Angew. Chem., Int. Ed.*, 2010, **49**(12), 2154–2157.

36 W. W. Yu and I. M. White, Inkjet-printed paper-based SERS dipsticks and swabs for trace chemical detection, *Analyst*, 2013, **138**(4), 1020–1025.

37 J.-U. Park, M. Hardy, S. J. Kang, K. Barton, K. Adair, D. k. Mukhopadhyay, *et al.* High-resolution electrohydrodynamic jet printing, *Nat. Mater.*, 2007, **6**(10), 782–789.

38 W. Fan, B. Shen, W. Bu, F. Chen, K. Zhao, S. Zhang, *et al.* Rattle-Structured Multifunctional Nanotheranostics for Synergetic Chemo-/Radiotherapy and Simultaneous Magnetic/Luminescent Dual-Mode Imaging, *J. Am. Chem. Soc.*, 2013, **135**(17), 6494–6503.

39 H.-S. Qian and Y. Zhang, Synthesis of Hexagonal-Phase Core–Shell NaYF4 Nanocrystals with Tunable Upconversion Fluorescence, *Langmuir*, 2008, **24**(21), 12123–12125.

40 F. Wang and X. Liu, Recent advances in the chemistry of lanthanide-doped upconversion nanocrystals, *Chem. Soc. Rev.*, 2009, **38**(4), 976–989.

41 S. Wu, N. Duan, X. Ma, Y. Xia, H. Wang and Z. Wang, A highly sensitive fluorescence resonance energy transfer aptasensor for staphylococcal enterotoxin B detection based on exonuclease-catalyzed target recycling strategy, *Anal. Chim. Acta*, 2013, **782**(0), 59–66.

42 B.-J. de Gans and U. S. Schubert, Inkjet Printing of Polymer Micro-Arrays and Libraries: Instrumentation, Requirements, and Perspectives, *Macromol. Rapid Commun.*, 2003, **24**(11), 659–666.

43 H. H. Lee, K. S. Chou and K. C. Huang, Inkjet printing of nanosized silver colloids, *Nanotechnology*, 2005, **16**(10), 2436–2441.

44 J. Mei, M. R. Lovell and M. H. Mickle, Formulation and processing of novel conductive solution inks in continuous inkjet printing of 3-D electric circuits, *Electron. Packag. Manuf., IEEE Trans.*, 2005, **28**(3), 265–273.

45 R. E. Saunders, J. E. Gough and B. Derby, Delivery of human fibroblast cells by piezoelectric drop-on-demand inkjet printing, *Biomaterials*, 2008, **29**(2), 193–203.

46 Y. Son and C. Kim, Spreading of inkjet droplet of non-Newtonian fluid on solid surface with controlled contact angle at low Weber and Reynolds numbers, *J. Non-Newtonian Fluid Mech.*, 2009, **162**(1–3), 78–87.

47 Y. Son, C. Kim, D. H. Yang and D. J. Ahn, Spreading of an inkjet droplet on a solid surface with a controlled contact

 This journal is © The Royal Society of Chemistry 2015

Published on 05 January 2015. Downloaded by Xian Jiaotong University on 30/05/2016 13:17:43.

angle at low Weber and Reynolds numbers, *Langmuir*, 2008, **24**(6), 2900–2907.

48 D. Xu, V. Sanchez-Romaguera, S. Barbosa, W. Travis, J. de Wit, P. Swan, *et al.* Inkjet printing of polymer solutions and the role of chain entanglement, *J. Mater. Chem.*, 2007, **17**(46), 4902.

49 Contributors W. HP Deskjet. 11 March 2014 07:31 UTC [cited; Available from: http://en.wikipedia.org/w/index.php?title=HP_Deskjet&oldid=599100789.

50 F. Wang and X. Liu, Upconversion Multicolor Fine-Tuning: Visible to Near-Infrared Emission from Lanthanide-Doped NaYF4 Nanoparticles, *J. Am. Chem. Soc.*, 2008, **130**(17), 5642–5643.

51 D. Ni, W. Bu, S. Zhang, X. Zheng, M. Li, H. Xing, *et al.* Single Ho3+-Doped Upconversion Nanoparticles for High-Performance T2-Weighted Brain Tumor Diagnosis and MR/UCL/CT Multimodal Imaging, *Adv. Funct. Mater.*, 2014, **24**(42), 6613–6620.

52 D. Ni, J. Zhang, W. Bu, H. Xing, F. Han, Q. Xiao, *et al.* Dual-Targeting Upconversion Nanoprobes across the Blood-Brain Barrier for Magnetic Resonance/Fluorescence Imaging of Intracranial Glioblastoma, *ACS Nano*, 2014, **8**(2), 1231–1242.

53 Y. L. Han, J. Hu, G. M. Genin, T. J. Lu and F. Xu, BioPen: direct writing of functional materials at the point of care, *Sci. Rep.*, 2014, **4**, 4872.

54 L. Tian, S. Tadepalli, M. E. Farrell, K.-K. Liu, N. Gandra, P. M. Pellegrino, *et al.* Multiplexed charge-selective surface enhanced Raman scattering based on plasmonic calligraphy, *J. Mater. Chem. C*, 2014, **2**(27), 5438–5446.

55 A. Russo, B. Y. Ahn, J. J. Adams, E. B. Duoss, J. T. Bernhard and J. A. Lewis, Pen-on-Paper Flexible Electronics, *Adv. Mater.*, 2011, **23**(30), 3426–3430.

56 K. A. Mirica, J. G. Weis, J. M. Schnorr, B. Esser and T. M. Swager, Mechanical Drawing of Gas Sensors on Paper, *Angew. Chem., Int. Ed.*, 2012, **51**(43), 10740–10745.